# Airwake Simulation of Modified TTCP/SFS Ship

**Tsze C. Tai***
Naval Surface Warfare Center, Carderock Division
Code 5300 West Bethesda, MD 20817-5700, USA
taitc@nswccd.navy.mil

**SUMMARY**

The TTCP/SFS ship configuration is modified by adding a rounded bow section at the front end to avoid complete separation along the side walls. Airwake of the modified configuration, subject to atmospheric wind of 70 ft/sec at wind angles of zero and 40 degrees, is simulated by using a multi-zone thin-layer Navier-Stokes method. The resulting flow contains regions of massive separation along with free vortices, but there is no separation along the hull surface observed. Major flow features including viscous-vortex interactions are captured. Large leading-edge separation coupled with leading-edge vortices at the front end of the round bow is detected. The flow then re-attaches over the forward deck. Calculated velocity data in the flight deck region will be made available to TTCP member activities upon request by e-mailing to the author.

## 1. INTRODUCTION

Recent work on airwake simulation based on the steady-state solution to Navier-Stokes equations provides reasonably accurate flowfield results that are useful to supplement experimental measurements, which otherwise would be more costly and time-consuming. A number of papers were presented at the last NATO RTO meeting in Amsterdam two years ago [1,3]. In particular, work on airwake of a special configuration, the Simplified Frigate Shape (SFS) as defined by The Technical Co-operative Program (TTCP) panel, is aimed at validating computational fluid dynamics (CFD) codes [4]. Simulated airwake results based on steady-state solution have been determined by Long et al [1] and Reddy et al [5]. Unfortunately, the SFS configuration has a flat nose that can have caused numerical difficulties that lead to discrepancies in comparison of results between the CFD simulations and wind tunnel tests. The present paper discusses drawbacks of the SFS ship, proposes a modification to the original configuration, and presents simulated airwake results over the modified ship.

The TTCP/SFS ship is shown in Fig. 1. The ship has a flat nose without bow. It causes numerical difficulties in solving the anticipated airwake flowfield. This configuration bears much resemblance

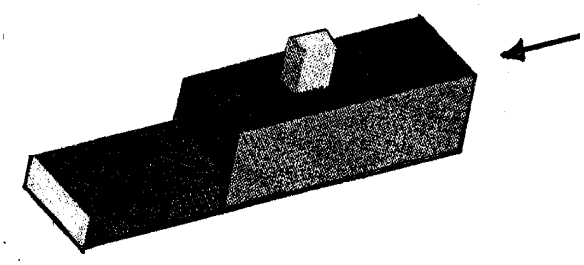

Fig. 1 -The Original TTCP/SFS Ship Configuration.

to the classic problem of flow over a flat nosed shape as illustrated in Fig. 2, which is taken from Schlichting's *Boundary Layer Theory* [6], As shown in Fig 2-(a), the flow past the fairly sharp corners in front caused suction followed by a large pressure increase along the side walls. This led to complete separation along the sidewalls, and to the formation of a wide wake behind the body. When the shape was changed by adding a round nose, the separation along the side walls were eliminated, see Fig. 2-(b).

---

* Senior Research Scientist, Marine and Aviation Department. Associate Fellow AIAA.

Presented at the NATO RTO Symposium on Vortex Flow and High Angle of Attack, Loen, Norway, 7-11 May 2001.

# Report Documentation Page

*Form Approved*
*OMB No. 0704-0188*

Public reporting burden for the collection of information is estimated to average 1 hour per response, including the time for reviewing instructions, searching existing data sources, gathering and maintaining the data needed, and completing and reviewing the collection of information. Send comments regarding this burden estimate or any other aspect of this collection of information, including suggestions for reducing this burden, to Washington Headquarters Services, Directorate for Information Operations and Reports, 1215 Jefferson Davis Highway, Suite 1204, Arlington VA 22202-4302. Respondents should be aware that notwithstanding any other provision of law, no person shall be subject to a penalty for failing to comply with a collection of information if it does not display a currently valid OMB control number.

| 1. REPORT DATE | 2. REPORT TYPE | 3. DATES COVERED |
|---|---|---|
| **00 MAR 2003** | **N/A** | **-** |

| 4. TITLE AND SUBTITLE | 5a. CONTRACT NUMBER |
|---|---|
| **Airwake Simulation of Modified TTCP/SFS Ship** | 5b. GRANT NUMBER |
| | 5c. PROGRAM ELEMENT NUMBER |
| 6. AUTHOR(S) | 5d. PROJECT NUMBER |
| | 5e. TASK NUMBER |
| | 5f. WORK UNIT NUMBER |
| 7. PERFORMING ORGANIZATION NAME(S) AND ADDRESS(ES) **NATO Research and Technology Organisation BP 25, 7 Rue Ancelle, F-92201 Neuilly-Sue-Seine Cedex, France** | 8. PERFORMING ORGANIZATION REPORT NUMBER |
| 9. SPONSORING/MONITORING AGENCY NAME(S) AND ADDRESS(ES) | 10. SPONSOR/MONITOR'S ACRONYM(S) |
| | 11. SPONSOR/MONITOR'S REPORT NUMBER(S) |

12. DISTRIBUTION/AVAILABILITY STATEMENT
**Approved for public release, distribution unlimited**

13. SUPPLEMENTARY NOTES
**Also see: ADM001490, Presented at RTO Applied Vehicle Technology Panel (AVT) Symposium held inLeon, Norway on 7-11 May 2001, The original document contains color images.**

14. ABSTRACT

15. SUBJECT TERMS

| 16. SECURITY CLASSIFICATION OF: | | | 17. LIMITATION OF ABSTRACT | 18. NUMBER OF PAGES | 19a. NAME OF RESPONSIBLE PERSON |
|---|---|---|---|---|---|
| a. REPORT | b. ABSTRACT | c. THIS PAGE | | | |
| **unclassified** | **unclassified** | **unclassified** | **UU** | **12** | |

**Standard Form 298 (Rev. 8-98)**
Prescribed by ANSI Std Z39-18

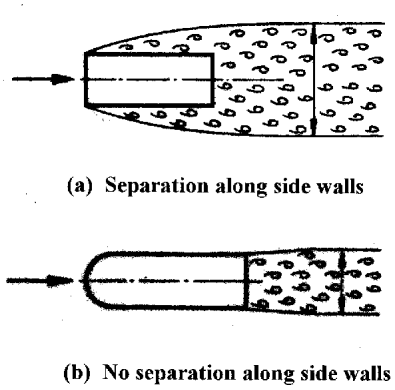

(a) Separation along side walls

(b) No separation along side walls

Fig. 2 - Classic flow about an angular versus round nosed model (Taken from Schlichting: *Boundary Layer Theory*)

## 2. MODIFIED TTCP/SFS CONFIGURATION

The flow over a body with complete separation is still a challenge for fluid dynamists, even with higher-order schemes and powerful computers. There is no adequate turbulence model for large, complete separation to date. One might be able to obtain plausible results on the original SFS ship, but their accuracy/validity is highly questionable. To overcome this shortcoming and computational difficulties involved in the original model, we propose here to add a rounded cylindrical bow section to the configuration. The modified SFS ship is shown in Fig. 3. The round bow eliminates the sharp corners in the shoulder between the nose and the main body, and thus reduces the separation and hence the numerical difficulties.

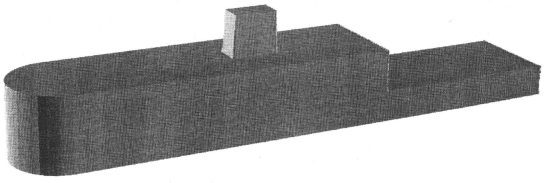

Fig. 3 – The Modified TTCP/SFS Configuration

Airwake of the modified configuration is simulated using a thin-layer Navier-Stokes method as described in the following section.

## 3. SIMULATION METHOD

The simulation method, or the computational method employed has been described previously [7,8]. For completeness, the method is briefly described here. It contains two main elements: 1) the grid generation and 2) the flow solving.

### 3.1 Grid Generation and Grid Topology

A structured, curvilinear, body-conforming grid is generated. Figure 3 in the previous section show the actual ship, i.e., the modified SFS configuration. The corresponding computational surface grid is shown in Fig. 4

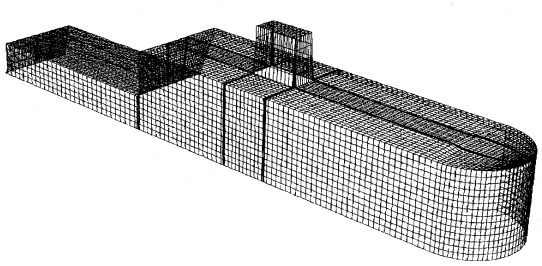

Fig. 4 - The Computational Mesh

The NASA Ames 3DGRAPE code [9] is used for basic grid generations. A cylindrical grid topology is adopted for its capability to treat a body with a sharp nose. The topology is basically an H-O mixed type, with H-type in the longitudinal plane, and O-type in the crossflow plane. The outer cylindrical surface is set at 2.5 ship lengths from the ship centerline. The most forward plane is set at 1.5 ship length from the bow of the ship, and 3.5 ship lengths for the wake in the rear of the stern.

A coarse grid for the flowfield is first generated by 3DGRAPE using a multi-block procedure. The radial distances are then clustered near the surface and stretched in the outer region for shear layer development. The complete grid has a total of 216 x 65 x 79 points with 79 points in the radial direction.

This mesh size is larger than those used for analysis of aircraft because of the very low speed freestream involved in the present work. Previous work [10] indicates that when using a compressible flow code at low Mach numbers, an increased mesh density is needed. The details of the grid generation and advantage of the grid topology adapted are presented in Ref. 11. The grid resolution has been improved by increasing the number of points in all three directions.

### 3.2 Flow Solver

The NASA Langley thin-layer Navier-Stokes code, the CFL3D code [12] with multi-zone capability, is used as the basic flow solver. Appropriate modifications to the code for applying specific boundary conditions are implemented. The code is based on a finite volume algorithm with a spatially factored diagonalized, implicit scheme for discretizing the three-dimensional, Reynolds-averaged Navier-Stokes equations. The upwind-biased differencing technique is used for the inviscid terms and central differencing for all viscous terms. The method is globally second-order accurate, well suited for patched grids in a multizone domain. Details are given by Thomas et al [12].

The code includes a variety of turbulence models, including the Baldwin-Lomax algebraic model, the one-equation models, and the standard two-equation models, among others. In the present work, two turbulence models are used: the Mentor $\kappa$ - $\omega$ two-equation model [13] and the B-L model [14]. The latter is used along with the Degani-Schiff modification [15] and the extension by Tai [16]. Tai extended the B-L model to 3-D flow by replacing the normal distance y in 2-D boundary-layer coordinates with the transverse arc length in 3-D curvilinear coordinates. Although simple, the B-L model has been regarded as the best turbulence model for flowfields dominated by vortical flow.

### 3.3 Boundary Conditions

The boundary conditions for the Navier-Stokes flow solver are: 1) atmospheric boundary layer flow upstream, 2) atmospheric pressure recovery downstream, 3) characteristic form of inflow-outflow at the cylindrical outer boundary, and 4) viscous nonslip flow at the surface of the ship. The atmospheric boundary layer is approximated by a power-law profile:

$$u/V_\infty = (z / h)^n \qquad (1)$$

where h is reference height and n varies from 0.10 to 0.14 [17]. The h is set to be the height of flight deck above the water surface, h = 0.104 ship length and n is set to its mean value of 0.12.

At the downstream boundary condition, instead of imposing the usual freestream recovery, the static atmospheric pressure condition is satisfied. In addition, velocity components are extrapolated from the interior. The use of characteristic form of inflow-outflow boundary condition at the cylindrical outer boundary is known to improve convergence of solution at low speed.

The water surface is assumed to be flat and waveless, and the flow properties in the airwake remain unmixed with the water. A reflective boundary is applied and the vertical velocity component must vanish at the water surface. This approach was reached after some other attempts at treating the water boundary failed. It turns out to be a good approximation.

## 4. RESULTS AND DISCUSSIONS

Numerical results of the flow over the modified TTCP/SFS ship configuration subject to an atmospheric wind speed of 32.7 m/s (70 ft/sec or 41 knots) and a wind direction of 0, and 40 degrees are obtained. The flow condition yields a Reynolds number of 117 million based on the ship length for the full scale ship. If the ship's beam were used for the Reynolds number basis, the above Reynolds number would have to be reduced approximately by a factor of 6. Whichever way the Reynolds number is calculated, the flow falls into the turbulent flow range. In addition, the results are rather insensitive to the different turbulence models employed.

All the computations were performed on the Cray facilities at the DoD High Performance Computing facility at the Naval Oceanographic Center (NAVO). Converged solutions were obtained in about 5,000 to 6,000 iterations (time steps) requiring approximately 30 to 36 hours of Cray SV1 CPU time. The large number of iterations is due to the very low freestream Mach number used in the compressible flow solver. The required CPU time is considered reasonable in today's environment of computer capability and resources.

### 4.1 Velocity Profile along Hull Surface

The primary purpose of the present modification of the TTCP ship configuration is to avoid complete separation about the configuration. The complete separation is characterized by total separation along the side walls of the vehicle, or the ship hull surface.

We determine whether there is flow separation by examining the velocity profile on the subject surface. Figure 5 shows the velocity profile along the hull surface from the tip of the bow. The flow is attached all the way along the hull surface. There is noticeable flow acceleration in the shoulder area, reaching a maximum velocity to 58 m/s (123 ft/sec), but there is no evidence of flow separation. In fact, this peaky velocity may attain enough momentum to keep the flow attached.

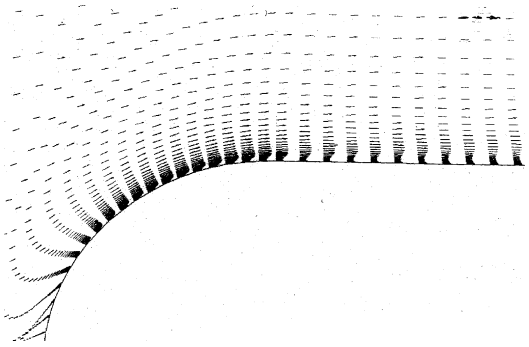

Fig. 5 – Velocity profile along the hull surface

### 4.2 Particle Traces

. The particle traces of the streamlines emanating from various stations on the ship surface for the case of the two wind directions, namely wind at zero, and 40 degrees with a speed of 32.7 m/s (70 ft/ses) are obtained. Figures 6 and 7 show the perspective view of the airwake particle traces, while Figs. 8 and 9 give the astern views of the same airwake over the ship. Even at zero wind angle, the figures all indicate that the flow is mostly separated virtually in all sections except the rear part of the fore deck.

There are two types of separation: one due to viscosity and the other due to sharp corners of the volume blocks representing the superstructure. The former is closely influenced by the types of flow involved which is Reynolds number dependent. The latter is purely an inviscid phenomenon, independent of the Reynolds number. Both types of separation create free vortices as evidenced by the streamlines rolling up forward and aft of the superstructure, on the rear flight deck, and aft of the stern. The mechanism of the vortical flow involving free vortices is well demonstrated by the present steady-state solution. The use of the Navier-Stokes method ensures the basic physical feature of the airwake, namely the three-dimensional flow separation which occurs over all the geometric surfaces, is captured.

The shape of the air burble (airwake) might be misleading in the perspective view. The burble is symmetric when the eyepoint is set at the center plane. Of course the height, as well as the overall size, of the air burble grows as the flow proceeds downstream. The height can be twice as much as shown here in about three ship lengths away. The airwake experiences a dip right aft of the stern. This is shown by the astern view in Fig. 7. The astern view also depicts how the airwake grows in size and shape.

. Figures 8 and 9 show the perspective and astern views of the particle trace over the modified TTCP ship at a wind angle of 40 degrees. The airwake becomes asymmetric at a wind angle of 40 degrees, see Fig. 8. Vortex rolling up takes place aft of the stern as a result of more severe flow separation generated by viscous-inviscid interactions. The region of separated flow is generally restricted to the port side of the ship. On the flight deck, the flow is massively separated as shown in Fig. 9.

There is still a low pressure region behind the superstructure which can influence the most portion of the flight deck, including the touch-down area (in the middle of the flight deck), see Fig. 9. The flow over and behind the superstructure exhibits characteristics of a 3-D backward facing step with massive flow separation involving reversed flow along with circulation. Rolling up of the vortex flow intensifies as depicted in Fig. 8. The leeside streamlines take off from the fore deck but swirl inward forming a strong vortex over the flight deck, see Fig. 9.

Moderate leading edge separation at the front end of the rounded bow is detected case of zero wind angles (Fig. 6), but become more severe as the wind angle increases (Fig. 8). The flow re-attaches over the forward deck where it decelerates due to presence of the superstructure.

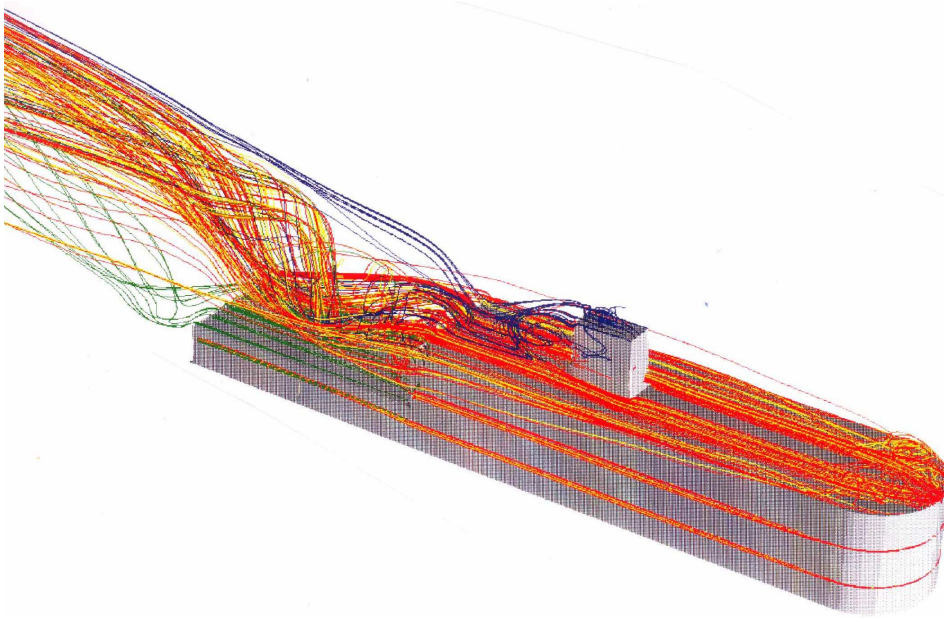

Fig. 6 - Particle Traces over Modified TTCP Ship at Even Keel at 32.7m/s (70 ft/sec) And Zero Wind Angle. Perspective View.

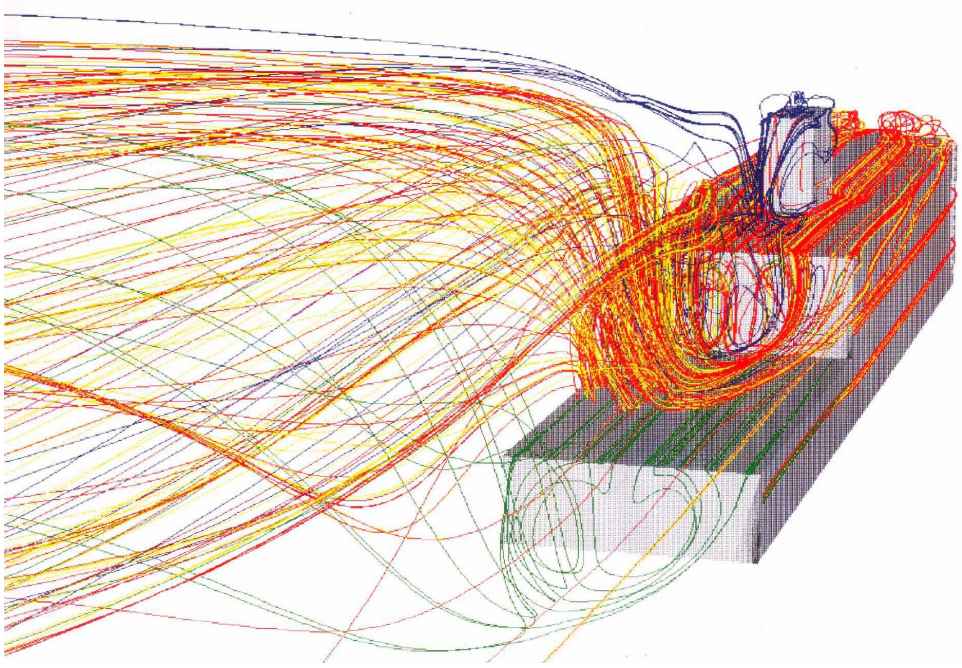

Fig. 7 - Particle Traces over Modified TTCP Ship at Even Keel at 32.7m/s (70 ft/sec) and Zero Wind Angle. Stern View.

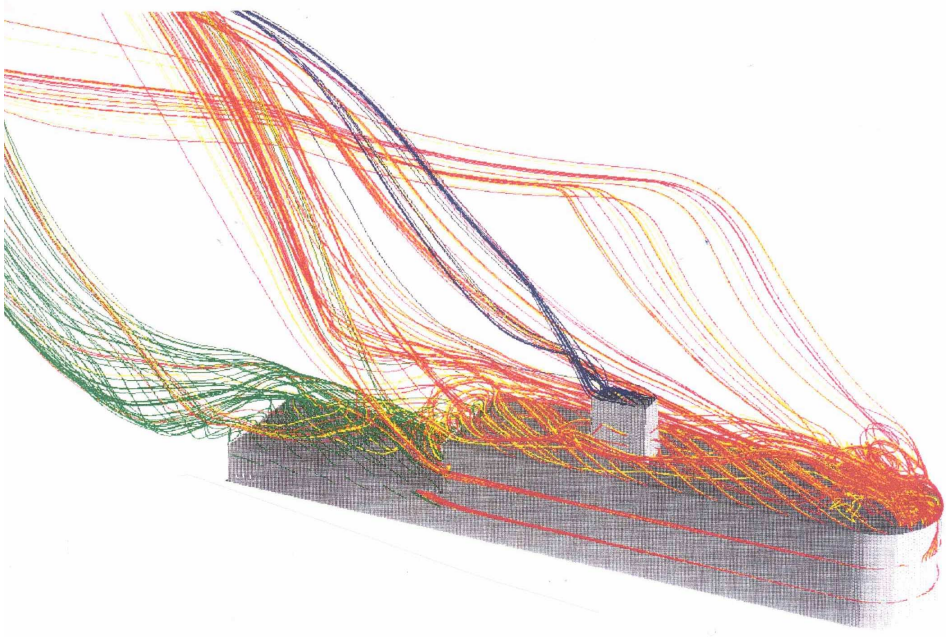

Fig. 8 - Particle Traces over Modified TTCP Ship at Even Keel at 32.7m/s (70 ft/sec) and 40-Deg Wind Angle. Perspective View.

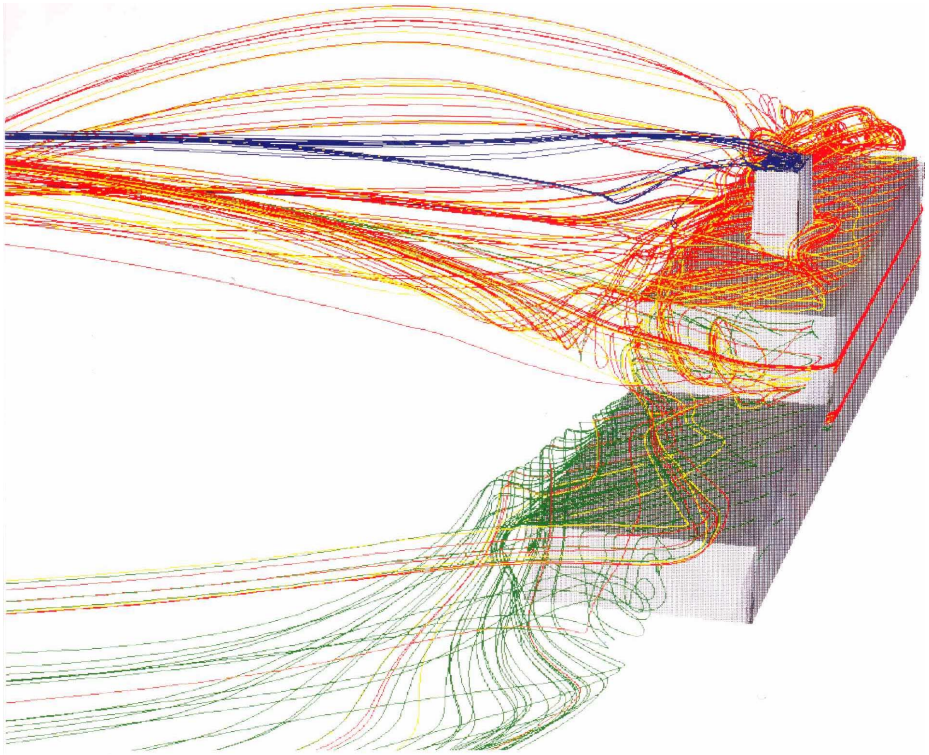

Fig. 9 - Particle Traces over Modified TTCP Ship at Even Keel at 32.7m/s (70 ft/sec) and 40-Deg Wind Angle. Stern View.

### 4.3 Velocity Vectors

The velocity vectors in the flight deck region of the modified TTCP ship are presented in Figs. 10 –11 for incoming wind speed of 32.7 m/s (70 ft/sec) at wind direction of 0 degrees.

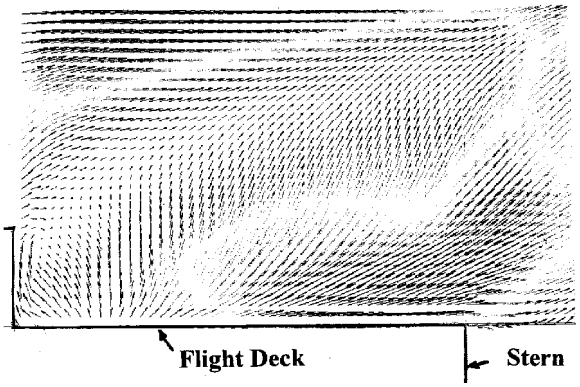


Fig. 10 – Velocity vectors along the center plane over the flight deck for wind speed at 32.7 m/s (70 ft/sec) and zero wind angle

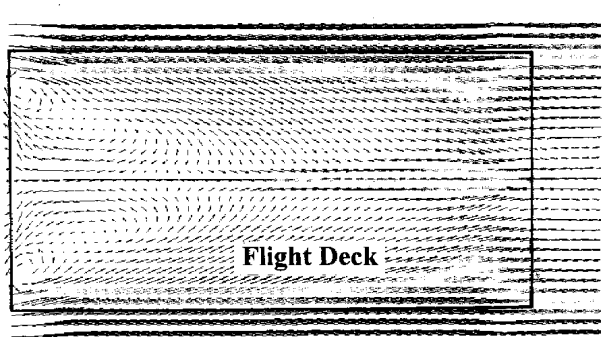


Fig. 11 – Velocity vectors in a horizontal plane 10 ft above the flight deck for wind speed at 32.7 m/s (70 ft/sec) and zero wind angle

Figure 10 shows the velocity vectors along the center plane over the flight deck. The magnitude of the velocity is proportional to the length of the arrow of each vector. The figure is reproduced from the original color-coded one that the velocity magnitude increases from blue to red with green and yellow in the middle. The light arrows are originally in yellow color representing median velocities. At the beginning of the flight deck, there is a re-circulation region immediately behind the hangar. The flow here is characterized by three-dimensional separation consisting of the vortex core and including positive vertical velocity components. These upward velocities result from the convergence of the flow from sides as evidenced in Fig. 11. There is a strong tendency that the flow converges from the edge of the deck toward the center and mixes with that from the hangar, forming a strong vortex field with massive separation.

Figures 12 and 13 show the velocity vectors along the center plane over the flight deck and in a horizontal plane above the deck for wind angle 40 degrees.

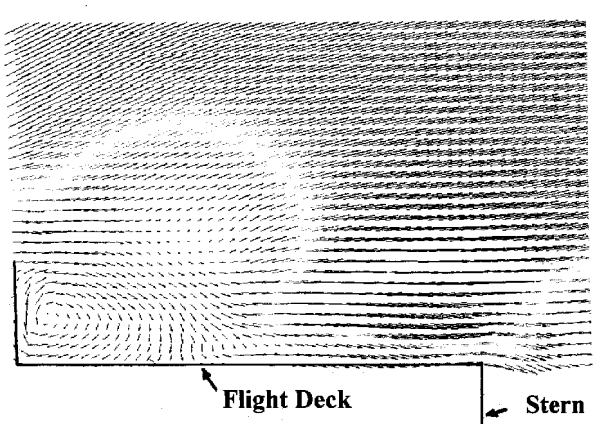


Fig. 12 – Velocity vectors along the center plane over the flight deck for wind speed at 32.7 m/s (70 ft/sec) and 40-deg wind angle

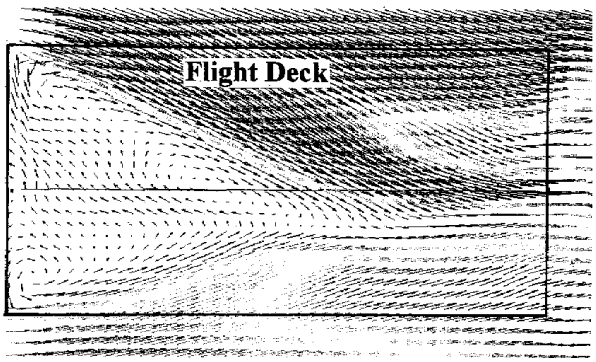


Fig. 13 – Velocity vectors in a horizontal plane 10 ft above the flight deck for wind speed at 32.7 m/s (70 ft/sec) and 40-deg wind angle

The increase in wind angle makes the flow become more involved with large velocity gradients and strong vortex fields. A strong vortex core is formed aft of the hangar. Large vertical velocities are replaced by some flow re-circulation near the middle of the deck, see

Fig. 12. For vectors in the horizontal plane 10 feet above the deck, Fig. 13, the flow is dominated by high velocities from starboard. Nevertheless, there is still flow emerging from the leeside (port side) towards the center, causing vortex-layer type flow separation due to convergence of streamlines. The line of separation is shifted towards the leeside of the plane.

Comparison of velocity vectors on the deck floor is made between the present results and those from Refs. 1 and 5, along with wind tunnel flow visualization data. These are shown in Figs. 14-17.

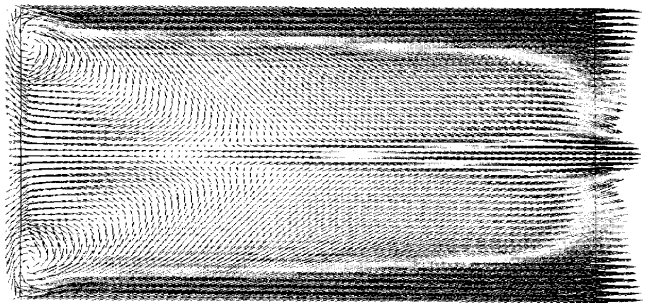

Fig. 14 – Velocity vectors on the flight deck floor for wind speed at 32.7m/s (70 ft/sec) and 0 wind angle (Present results, Re = 117 million)

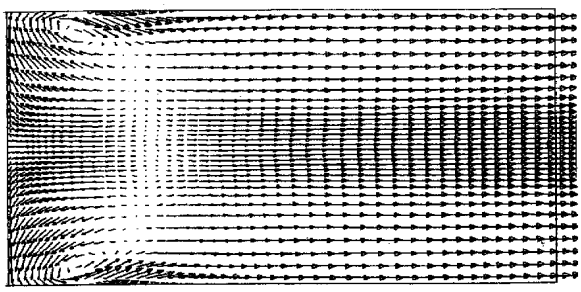

Fig. 15 – Velocity vectors the flight deck floor for wind speed at 32.7m/s (70 ft/sec) and 0 wind angle (Ref. 5, Re = 15 million)

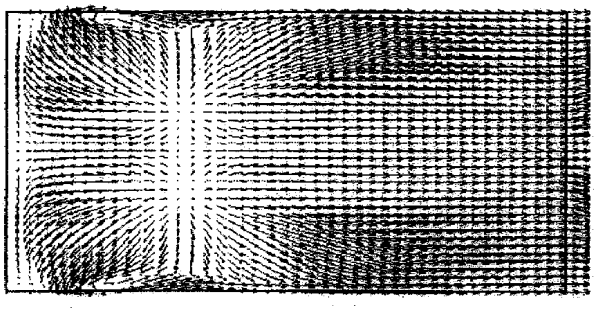

Fig. 16 – Velocity vectors on the flight deck floor for wind speed at 32.7m/s (70 ft/sec) and 0 wind angle (Ref. 1, Re = 15 million)

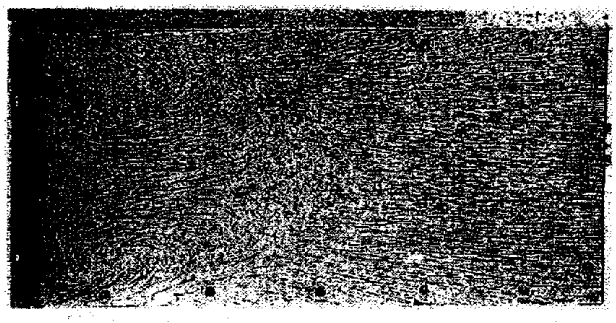

Fig. 17 – Velocity vectors the flight deck floor for wind speed at 32.7m/s (70 ft/sec) and 0 wind angle (Wind-tunnel flow visualization, Re = 0.85 million)

The Reynolds number used in the present work is 117 million based on full length of the ship, while in Refs. 1 and 5, the Reynolds number is 15 million based on the ship beam, whereas it is about 0.85 million for the wind-tunnel test. They are all in the range of fully developed turbulent flow, so it is generally considered that the flow field is not too sensitive to the effect of Reynolds number.

The present results predict reasonably well the main features of the flow including the two vortex cores at the rear of the hangar. However, the size of the re-circulation zone and the location of the vortex pair differ from the experimental data. These differences could be due to the fact that present results were based on the modified configuration while the wind-tunnel data were obtained using the original

TTCP ship that had flat blunt front end. After the complete separation due to flat front end, it is possible that the flow might re-attach somewhere downstream, but this would have altered the overall flow characteristics of the airwake flowfield. Computational results of Refs. 1 and 5 were also based on the original TTCP ship. However, it is not clear whether these results involve in a complete separation along the sidewalls (hull surface).

Plots of velocity vectors over the forward deck (not shown) indicate large flow separation in the leading edge region due to sharp edge. This is consistent with the leading edge separation bubble seen in the particle traces (Figs 6 and 8). Similarly, flow separation takes place over the superstructure because of its front sharp edge. Removing those sharp edges through further modification of the ship could eliminate these separations.

### 4.4 Velocity Distributions

The particle traces and velocity vectors offer visual insights the simulated airwake flowfield whether it contains the correct physics it should have. The usefulness of the resulting airwake, however, depends on the ability to provide the correct velocity distributions needed to define the flight envelope for aircraft shipboard operation. Here we examine the velocity components U, V, W in a region above the flight deck starting from the rear of the hangar to one flight-deck length aft of the stern. These velocity components would be useful for flight envelope analysis. The layout of the region is shown in Fig. 18 below.

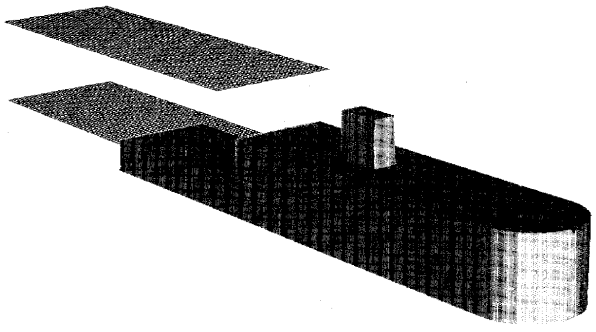

.

Fig. 18 – Layout of the region for velocity distributions

The distribution region consists of a rectangular volume of the size 90 feet long, 60 feet wide, and 40 feet high. Values of velocity components u,v,w are interpolated in every two feet along three Cartesian coordinates x,y,z.. Figure 19 presents results of the velocity distributions 10 feet above the flight deck (25 feet above the water level) at an x = 45 feet from the hangar. The plane corresponds to the Section B

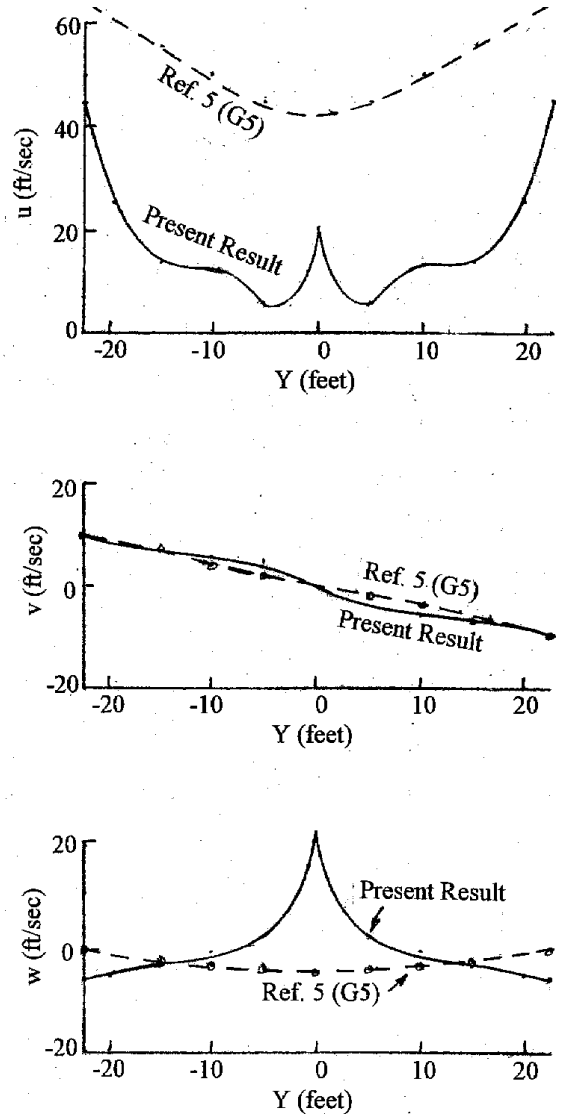


Fig. 19 – Velocity distributions in a plane above the flight deck for wind speed at 32.7 m/s (70 ft/sec) and zero wind angle.

as defined in Ref. 5. Three velocity components u,v,w are plotted. Large velocity deficit in the longitudinal velocity u is mainly due massive flow separation in the rear of the hangar. The flow converges from the deck edges towards the center plane, resulting in large positive vertical velocity w at the center. The physical phenomenon is known as classical three-dimensional flow separation in which the separation line is found below the line of convergence. It is the converging

fluids force the flow to leave the surface without the skin friction being vanished at wall.

Comparison of the present results and those of Ref. 5 reveals significant deviations in both longitudinal and vertical components between the two methods, while close correlation in the crossflow velocity is observed.

Figure 20 shows the distribution of the u component velocity in a vertical plane over the flight deck at x = 45 feet from the hangar. The values of u are indicated on the chart in feet per second. The velocity declines from the edge inward, resulting in a negative velocity region area near the center. The horizontal line lies 10 feet above the deck or 25 feet above the water level where the u values are shown in the top of Fig. 19.

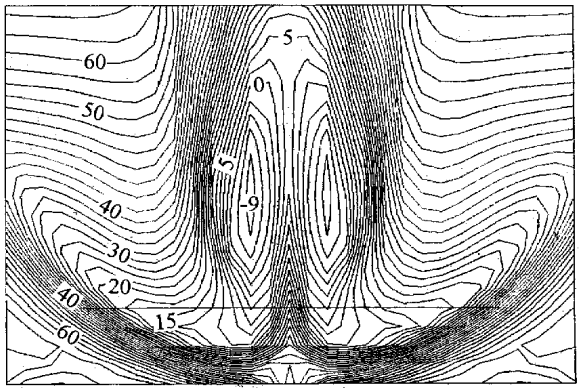


Fig. 20 – Distribution of u-component velocity in a vertical plane above the flight deck, 45 feet from the hangar. (Numerical numbers are values of u velocity in ft/sec.)

Since the purpose of the TTCP/SFS ship is for comparison of the CFD data and experimental measurements among its member countries, we will make the velocity distribution data as defined in the above region available to the TTCP member organizations. Request for the data should be made by sending an e-mail to the present author at taitc@nswccd.navy.mil. The data will also be made available to none TTCP member activities upon approval by the US Navy.

## 5. CONCLUDING REMARKS

The airwake of the modified configuration, subject to atmospheric wind of 32.7 m/s (70 ft/sec) at wind angles of zero and 40 degrees, is simulated by using a multi-zone thin-layer Navier-Stokes method. The resulting flow contains regions of massive flow separation along with free vortices. Major flow features including viscous-vortex interactions are captured. Some concluding remarks may be drawn from the results of this study:

(1) By modifying the TTCP configuration to include a rounded bow, complete separation along the hull surface is avoided.

(2) The flow over and behind the superstructure has characteristics of a 3-D backward facing step with massive flow separation involving reversed flow along with circulation.

(3) Large leading edge separation at the front end of the rounded bow is detected. The flow re-attaches over the forward deck where it decelerates due to presence of the superstructure.

## 6. ACKNOWLEDGMENT

The present work was supported by the Research Venture Program at NSWC, Carderock Division under the cognizance of J. Barkyoumb. The DoD High Performance Computing facility located at Naval Oceanographic Center provided the supercomputer CPU time.

## 7. REFERENCES

[1] Long, L.N., Liu, J, and Modi, A.V., "Higher Order Accurate Solutions of Ship Airwake Flow Fields Using Parallel Computers," Paper No. 3, *Proceedings of NATO RTO Meeting on Fluid dynamics Problems of Vehicles Operating Near or in the Air-Sea Interface,* RTO-MP-15, Neuilly-Sur-Seine Cedex, France, February 1999.

[2] Tai, T.C., "Simulation and Analysis of LHD Ship Airwake by Navier-Stokes Method," Paper No. 4, *Proceedings of NATO RTO Meeting on Fluid dynamics Problems of Vehicles Operating Near or in the Air-Sea Interface,* RTO-MP-15, Neuilly-Sur-Seine Cedex, France, February 1999.

[3] Zan, S.J., Syms, G.F., and Cheney, B.T., "Analysis of Patrol Frigate Air Wakes," Paper No. 7, *Proceedings of NATO RTO Meeting on Fluid dynamics Problems of Vehicles Operating Near or in the Air-Sea Interface,* RTO-MP-15, Neuilly-Sur-Seine Cedex, France, February 1999.

[4] Wilkinson, C.H., Zan, S.J., Gilbert, N.E., and Funk, J.D., "Modeling and Simulation of Ship Air Wakes for Helicopter Operations -- A Collaborative Venture," Paper No. 8, *Proceedings of NATO RTO Meeting on Fluid dynamics Problems of Vehicles Operating Near or in the Air-Sea Interface,* RTO-MP-15, Neuilly-Sur-Seine Cedex, France, February 1999.

[5] Reddy, K.R., Toffoletto, R., Jones, K.R.W., "Numerical Simulation of Ship Airwake," *Computers & Fluid*, Vol. 29, 2000, pp.451-465.

[6] Schlichting, H., "*Boundary Layer Theory*," 4th edition translated by Dr. J. Kestin, McGraw-Hill, New York, 1962. Page 34.

[7] Tai, T.C. and Carico, D., "Simulation of DD-963 Ship Airwake by Navier-Stokes Method," *Journal of Aircraft*, Vol. 32, No. 6, Nov-Dec 1995, pp. 1399-1401.

[8] Tai, T.C., "Simulation of LPD Ship Airwake by Navier-Stokes Method," *Proceedings of the Sixth Asian Conference on Fluid Mechanics*, Vol. II, Singapore, 1995, pp. 1620-1624.

[9] Sorenson, R.L., "The 3DGRAPE Book: Theory, Users' Manual, Examples," NASA Technical Memorandum 102224, Jul 1989.

[10] Volpe, G, "On the Use and Accuracy of Compressible Flow Codes at Low Mach Numbers," AIAA Paper 91-1662, June 1991.

[11] Tai, T.C., "A Single Structured Grid for Complex Ship Geometry," in *Numerical Grid Generation in Computational Fluid Dynamics and Related Fields*, Edited by N.P. Weatherill, Pineridge Press Limited, Swansea, U.K. Apr 1994.

[12] Thomas, J.L., Krist, S.T., and Anderson, W.K., "Navier-Stokes Computations of Vortical Flows over Low-Aspect-Ratio Wings," *AIAA Journal*, Vol. 28, No. 2, 1990. Pp. 205-212.

[13] Menter, F., "Improved Two-Equation $\kappa$ - $\omega$ Turbulence Models for Aerodynamic Flows," NASA TM 103975, 1992.

[14] Baldwin, B.S., and Lomax, H., "Thin-Layer Approximation and Algebraic Model for Separated Turbulent Flows," AIAA Paper 78-0257, Jan 1978.

[15] Degani, D., and Schiff, L.B., "Computation of Supersonic Viscous Flows Around Pointed Bodies at Large Incidence," AIAA Paper 83-0034, 1983.

[16] Tai, T.C., "Extension of Baldwin-Lomax Turbulence Model to Three-Dimensional Flow," AIAA Paper 97-0209, Jan 1997.

[17] Plate, E.J., *Engineering Meteorology*, Elsevier Scientific Publishing Co., Amsterdam, 1982, pp. 527-569.

**Paper: 26**
**Author: Dr. Tai**

**Question by Dr. Luckring**: What turbulence model was used?

Answer: Both modified Baldwin-Lamax model and Menter's k-ω SST model were needed. Results are pretty close to each other.

Question 2: Were results shown steady or unsteady?

Answer: Results are based on the steady-state solution to the Navier-Stokes equations, so there is no unsteadiness involved.

Question 3: Are there data to compare your results against?

Answer: There are no experimental data available yet for this brand new configuration to compare the calculated results against. However, calculated flow patterns over the flight deck compare qualitatively well with wind-tunnel data from the Naval Post Graduate School for a similar deck and also with a full-scale test from an Australia lab.

Question 4: Could you contrast your approach to that of Paper #25 by Ms. Polsky?

Answer: The present paper uses the steady-state solution to the N-S equations while Paper #25 uses the unsteady solution.